



## Valorization of banana peel and waste cooking oil to prepare biogreases

Refaat A. El-Adly<sup>a,b</sup>, Abdulraheem S. Almalki<sup>a</sup>, Maram J. ALzhrani<sup>a</sup>, Hussien A. Elmawgoud<sup>b</sup>, Dalia M. Abbas<sup>b</sup>

<sup>a</sup> Chemistry Department, Faculty of Science, Taif University, KSA

<sup>b</sup> Egyptian Petroleum Research Institute, Nasr City, Cairo, Egypt



### Abstract

In general lubricating greases contain mineral oil as fluids, which are toxic to the environment after use. On the other hand, waste cooking oil is discarded in sewage, and banana peel is dumped in landfills; this waste has created a negative impact on the environment and economy. Accordingly, the objective of this study is to prepare biogrease from waste cooking oil and banana peel. Purification and improvement of these wastes were carried out respectively; their physical and chemical properties were determined using advanced analytical tools. Also, the kinetic analysis of the thermal degradation of banana peel was obtained from weight loss at temperatures (0-800°C) using model-free, modelistic methods and MATLAB; it showed all the possible mechanisms have a non-isothermal modelistic method. Five formulations from biogreases were prepared based on banana peels and waste cooking oil; the physicochemical properties of this formulation were determined. It was shown that the dropping point and consistency of grease depend on the ratio of banana peels incorporated in the grease formulation. The use of a blend of lithium soap and banana peels as thickeners provides properties comparable to that found for commercial lithium grease. It was concluded that the waste cooking oil and banana peel can offer promising eco-friendly raw materials for the production of biogrease.

**Keywords:** Vegetable oil; Agriculture waste; Cooking oil; Banana peels Management; Biogrease; Lithium grease; Kinetics analysis.

### 1. Introduction

Currently, one of the main priorities in fuel and energy management is the quest for ecologically benign materials that could replace mineral oil in a variety of industrial applications. This is mostly because of the world's fossil fuel sources being depleted so quickly and because people are becoming more conscious of the environmental damage caused by the excessive use and disposal of mineral oil. Lubricating greases are regarded as thickening colloidal dispersions in lubricating fluids. Their ability to lubricate and biodegrade depends on both the thickening and base oil [1]. Because it reduces friction between mechanical parts, lubricating grease is utilised in a wide range of machine applications [2]. Grease is not biodegradable and is primarily made from basic materials derived from petroleum.

Many scientists have created bio lubricants from virgin vegetable oils including soy bean oil, castor oil, rapeseed oil, palm oil and jojoba oil, scientists have created biolubricants [3–7]. There is a need for an affordable and environmentally beneficial alternative to virgin oil since in the case of biolubricants made from these oils, 80–90% of the production costs are attributed to virgin oil as a raw material. Therefore, scientists are working on low-cost, readily accessible, and environmentally benign ways to produce biolubricants, such as biogreases, from leftover cooking oil [8–10]. So, waste cooking oil has attracted great attention since it is regarded as a sustainable source for making affordable biolubricants [11].

Although, it has some changes in physical and chemical properties, due to frying but it exhibits other properties of

vegetable oil [12]. Waste cooking oil with antioxidants was investigated to prepare sustainable biolubricants formulation [13]. Conversely, one of the most important crops in the world is the banana. Over 116 million tons of bananas were produced worldwide in 2019 [14]. Peels from bananas are a plentiful waste product; for every 10 tons of bananas, one ton of garbage is generated [15]. Waste management results from the discarding of banana peel, which makes up roughly 40% of the weight of the banana [16]. Banana peels are a viable waste material for the industry since they are high in dietary fibers, proteins, carbs, and mono- and disaccharides, and they contain 20–30% fiber. Banana peels can be converted enzymatically, mechanically, or chemically into products with additional value. They are relatively inexpensive, easily accessible, lightweight, and environmentally acceptable material [17].

In this respect, Waste valorization involves transforming waste materials into fuels and lubricants, among other more beneficial goods. The rapidly depleting natural and primary resources make waste valorization a necessity for sustainable and affordable waste management solutions rather than a luxury for academic research. Due to its high cost, biogrease cannot economically compete with lubricating greases based on petroleum [18–19].

In this way, the present study aims to identify, upgrade, and utilization of waste cooking oil and banana peel to prepare biogreases. The formulation of biogrease from these wastes is completed by mixing and homogenizing methods with the variation of the biogrease ingredients

\*Corresponding author e-mail: [dalia.epri@yahoo.com](mailto:dalia.epri@yahoo.com) (Dalia M. Abbas)

Receive Date: 29 April 2024, Revise Date: 27 June 2024, Accept Date: 21 July 2024

DOI: 10.21608/ejchem.2024.286060.9659

©2024 National Information and Documentation Center (NIDOC)

and by introducing an additive to improve particular properties of the formulated biogrease.

## 2. Materials and analysis techniques

### 2.1. Waste cooking oil (WCO)

The used WCO in this study was collected from Taif University restaurant. Solid particles and impurities were separated from WCO by filtration using filter paper; then purification through treated with superfast M2FF bleaching earth (highly active acid bleaching earth, AMCOL); After purification, the oil obtained is known as PWCO. The obtained PWCO was kept in a sealed bottle before use to avoid contamination and reaction with air. The PWCO was analyzed to evaluate the physicochemical properties according to the American Standard for Testing and Methods. A DB-23 column (60 m × 0.25 μm) with an Agilent 6890 series GC system was used to analyse the fatty acid contents of PWCO. Methyl ester was prepared from fatty acids and then injected straight into the GC. N<sub>2</sub> was the carrier gas, and it had a splitting ratio of 1:80 and a flow rate of 2.2 ml/min. The temperature of the FID detector was 270°C, whereas the injector was 250°C. The temperature was adjusted as follows: it was held at 225°C for 20 minutes after rising to 225°C at a rate of 50°C per minute. A Perkin-Elmer FTIR Spectrum BX spectrophotometer was used to determine the function groups in purified waste cooking oil. The range of 4000–450 cm<sup>-1</sup> was used to acquire the infrared data [4,20].

### 2.2. Banana peel collection and preparation

The banana peels that were used collect from a local fruit market. To get fragile fully dried portions, it was first sliced into little pieces and allowed to dry for five days outside. Next, it was deep dried for twenty-four hours at 110°C in a laboratory oven using Binder tools. The dried banana peel that is obtained is called DBP. Ultimately, a ball mill was used to grind the peels that had been deep-dried (PULVERISETTE5). After that, the peels were sealed, put through a 375 mesh filter, and kept at room temperature in the laboratory [21]. The chemical compositions of banana peel including, cellulose, hemicellulose, lignin, and ash were determined using gravimetric methods [21]. The quantitative elemental analysis of banana peel was conducted using an energy-dispersive X-ray fluorescence spectrometer (QuantX EDXRF, Thermo Fisher Scientific Inc., USA). The topography determination of both BP and DBP was evaluated using an SEM (JOEL, Model: JSM-5600,

Japan.) attached with a secondary electron detector picked up at magnifications x 2700 (5 μm) and x 270 (50 μm).

Thermo Analytical DTA paired with TGA model SETSYS Evolution-1750 SETARAM apparatus was used to do thermal analysis on banana peels throughout a temperature range of 25 to 1000°C in a nitrogen atmosphere. The sample weighed 20 mg. The heating rate was set at 10 °C/min. Nitrogen was pumped out of the sample at a 100 mL/min flow rate. During the analysis, the material was kept in sealed, hermetic aluminium pans with a cooling rate of 5°C per minute.

### 2.2.1. Kinetic analysis

Kinetic analysis of the thermal degradation of banana peel was investigated based on weight loss at temperatures (0-800°C) using model-free, modelistic methods and MATLAB.

### 2.3. Biogrease preparation

Five formulations of biogrease designated G1 to G5 were prepared according to formulated ratios based on PWCO, Dried banana peels, stearic acid, lithium hydroxide, styrene-butadiene rubber, and dodecyl amine as mentioned in Table 1. The prepared biogreases were prepared in batches of one liter in an autoclave with a capacity of 2 liters, fitted with a mechanical stirrer. The autoclave was charged with the ingredients for each type as described elsewhere [4,22]. The mixture of PWCO, stearic acid, and required lithium hydroxide was stirred at 100 rpm for 1-2 hours at a temperature of 180°C to saponification then cut back with additional PWCO.

A sample is then taken to ensure that the saponification process is completed in situ by determining total acidity. The required PWCO, DBP, and their additives (Styrene butadiene rubber as a viscosity modifier & dodecyl amine as an antioxidant) were added as needed to produce the desired consistency of biogrease; then it homogenized using a colloidal mill after the temperature was allowed to cool to room temperature. The physicochemical properties of the obtained biogreases G1 to G5 were determined according to ASTM methods, and compared with commercial lithium grease designated G6. Moreover, the anti-wear properties of the formulated biogreases compared with G6 were evaluated using a pin-on-disc apparatus as reported elsewhere [22]. The weight loss of pins before and after were calculated and estimated the volume wear loss in cubic millimeters (density of pin is 7.73 gm/cm<sup>3</sup>) to evaluate the efficiency of formulated biogreases and commercial ones.

**Table 1: Ingredients of the formulated prepared biogreases**

Formulated biogrease Ingredient, wt%	G1	G2	G3	G4	G5
Purified waste cooking oil	71.0	68.0	63.0	61.3	58.3
Stearic acid	15.0	14.0	13.0	10.0	8.0
lithium hydroxide	1.2	1.0	0.8	0.9	0.9
Dried Banana peels	10	15	20	25	30
Styrene butadiene rubber	2.5	2.5	2.5	2.5	2.5
dodecyl amine	0.3	0.3	0.3	0.3	0.3

## 3. Result and discussion

To manage biomass waste to convert it into a material resource and to upgrade and utilize area lubricant or energy, considerable efforts are being studied [4-6,22]. To prepare biogrease from PWCO and Dried banana peel as raw materials, the identification and characterization were focused on in the following section.

### 3.1. Physicochemical properties of PWCO

The WCO under investigation was purified according to the methodology described in the experimental section. As a result, as shown in Table 2, the physicochemical characteristics of the purified waste cooking (PWCO) oil were determined by applying ASTM/IP standard test procedures. The data indicates that PWCO has a kinematic viscosity of 8.16 cSt at 100°C, indicating that it is a suitable fluid to employ in the preparation of

lubricating greases. The peroxide value and total acid number of PWCO were 5.5 and 1.85 respectively. The oxidation stability index and iodine value are 11 and 85 respectively. These results explain the hydrolysis, thermal oxidation, and polymerization reactions that happened

during the frying process. Data here are similar to those reported earlier [22] and agree with results reported by other researchers, who conducted detailed analyses of WCO [23].

**Table 2: Physicochemical properties of PWCO**

Characteristics	PWCO	Test
Density, g/ml at 25/25°C	0.863	ASTM D.1298
Refractive index, n <sub>20</sub> °C	1.4652	ASTM D.1218
Kinematics viscosity, c St. at 100°C	8.16	ASTM D.445
Dynamic Viscosity, at 50°C (rpm 30), Cp	80	ASTM D.97
TAN, mg KOH/gm	1.85	ASTM D-664
Average Molecular weight	640	GPC
Iodine value	85	ASTM D-5554
Oxidation stability index	11	Cd 12b-92
Peroxide value	5.5	ISO 3960

Table 3 presents the analytical data on the fatty acid composition of purified waste cooking oil using a gas chromatography technique. The fatty acids that have been detected in WCO are as follows: capric, lauric, tridecanoic, myristic, pentadecanoic, palmitic, palmitoleic, heptadecanoic, stearic, and oleic, with percentages of 0.66, 0.43, 0.28, 19.30, 4.96, 22.94, 8.29, 8.63, 4.95, 0.66, and 0.43%, respectively.

This indicates that the main fatty acids were palmitic and myristic and that the possibilities of PWCO are under investigation as an alternative to be used in lubricant formulation. The IR spectrum of PWCO is shown in Figure 1. It shows the intense absorbance bands of the

PWCO can be shown in the range 440- 4000 cm<sup>-1</sup>. The doublet bands at 2991 cm<sup>-1</sup> and 2854 cm<sup>-1</sup>, absorptions are characteristic of the asymmetrical and symmetrical vibrations of the CH<sub>2</sub> and CH<sub>3</sub> aliphatic groups in the triglycerides of PWCO, while band 3004 cm<sup>-1</sup> could be predominantly arising from unsaturation fatty acid, mainly linoleic acid. The appearance strong band at 1743 cm<sup>-1</sup> may attributed to the carbonyl group which is associated with triglycerides or the presence of oxidation products such as aldehydes, ketones, and carboxylic acids, due to the frying process of oil.

**Table 3: Fatty acid composition of PWCO**

Common name	Fatty Acid	Chemical formula	Purified waste oil
Capric acid	C10	CH <sub>3</sub> (CH <sub>2</sub> ) <sub>8</sub> COOH	3.66
Lauric acid	C12	CH <sub>3</sub> (CH <sub>2</sub> ) <sub>10</sub> COOH	1.83
<a href="#">Tridecanoic acid</a>	C13	CH <sub>3</sub> (CH <sub>2</sub> ) <sub>11</sub> COOH	0.28
<a href="#">Myristic acid</a>	C14	CH <sub>3</sub> (CH <sub>2</sub> ) <sub>12</sub> COOH	25.30
Pentadecanoic acid	C15	CH <sub>3</sub> (CH <sub>2</sub> ) <sub>13</sub> COOH	5.96
<a href="#">Palmitic acid</a>	C16:0	CH <sub>3</sub> (CH <sub>2</sub> ) <sub>14</sub> COOH	27.00
Palmitoleic acid	C16:1	CH <sub>3</sub> (CH <sub>2</sub> ) <sub>14</sub> COOH	10.30
Heptadecanoic acid	C17	CH <sub>3</sub> (CH <sub>2</sub> ) <sub>15</sub> COOH	10.63
<a href="#">Stearic acid</a>	C18:0	CH <sub>3</sub> (CH <sub>2</sub> ) <sub>16</sub> COOH	5.95
<a href="#">Oleic acid</a>	C18:1	CH <sub>3</sub> (CH <sub>2</sub> ) <sub>7</sub> CH=CH(CH <sub>2</sub> ) <sub>7</sub> COOH	6.66
<a href="#">Linoleic acid</a>	C18:2	CH <sub>3</sub> (CH <sub>2</sub> ) <sub>4</sub> CH=CHCH <sub>2</sub> CH=CH(CH <sub>2</sub> ) <sub>7</sub> COOH	2.43

The stretching vibration of the methylene group ( $\delta$ CH<sub>2</sub>) is indicate for the strong band that was seen at 1511 cm<sup>-1</sup>. Several strong bands were identified in the fingerprint region between 1511 cm<sup>-1</sup> and 1104 cm<sup>-1</sup>, which can be attributed to the -CH<sub>2</sub> scissoring vibration at 1456 cm<sup>-1</sup>, the bending vibration of the HCH symmetric at 1367 cm<sup>-1</sup>, the bending or stretching vibrations of the CH<sub>2</sub> at 1,237 cm<sup>-1</sup>, the wagging vibration of the CH<sub>2</sub> at 1157 cm<sup>-1</sup>, and the stretching vibration of the C-O at 1104 cm<sup>-1</sup>. The distinctive bands located at 955 cm<sup>-1</sup>, 862 cm<sup>-1</sup>, and 719 cm<sup>-1</sup> are refer to the H-C-C and CH<sub>2</sub> rocking vibrations of PWCO that are being examined.

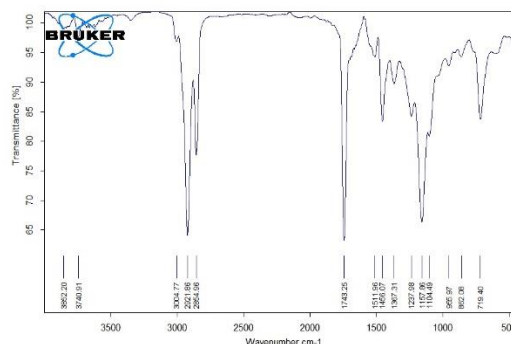


Figure 1: FTIR Spectrum of PWCO

### 3.2. Banana peel identification

#### 3.2.1 Chemical composition

Table 4 provides the chemical composition of the banana peel that is being examined; It demonstrates that lignocellulose, which is a compact structure comprising cellulose (22%) and hemicellulose (47%) in close proximity to lignin-substituted phenyl propane in three-dimensional polymers linked together by ether linkages (19.5%) and ash (11.5%), is the primary constituent of BP. These results exclude moisture content and consider that the main components after drying are lignin, cellulose, hemicellulose, and ash content. It may be mentioned that the chemical composition of BP depends on the species, climate, and geographical location.

**Table 4: Chemical composition of banana peel: Component Percentage (%)**

Component	Percentage (%)
Lignin	19.5
Cellulose	22.0
Hemicellulose	47.0
Ash	11.5

Figure 2 shows the FTIR spectrum of banana peel, which was recorded between 4000-400  $\text{cm}^{-1}$ . The lignocellulosic compounds of BP under investigation are represented by their chemical structure in this figure. It has a wide band at 3500-3100  $\text{cm}^{-1}$ , centered at 3285, which can be attributed to the hydroxyl groups in the aliphatic and phenolic structures of the composition of lignin. Hydrogen bond vibrations in cellulose's inter- and intra-molecular bonds are also included in this peak. The CH stretching in the aromatic methoxyl groups of the lignin molecule may be the main source of the signal centered at 2923  $\text{cm}^{-1}$ . Unconjugated carbonyl/carboxyl, which might result from the stretching vibration of lignocellulosic substances, is believed to be the source of the prominent band with a center of 1725  $\text{cm}^{-1}$ .

There detected a little vibration at 1244  $\text{cm}^{-1}$ , which is related to the stretching of the cellulose complex C-C and

C-O. Furthermore, in addition to the aromatic ring vibration, the C-H deformation and the aromatic skeleton vibration may be the cause of the spectral bands centered at 1374  $\text{cm}^{-1}$  and 1594  $\text{cm}^{-1}$ , respectively. The strong band at 1025  $\text{cm}^{-1}$  is caused by the aromatic C-H deformation, a complex vibration associated with the C-O, C-C stretching, and C-OH bending in polysaccharides. The H-C-C or  $\text{CH}_2$  rocking vibrations mode in cellulosic compounds could be attributed to the vibration band at 770  $\text{cm}^{-1}$ .

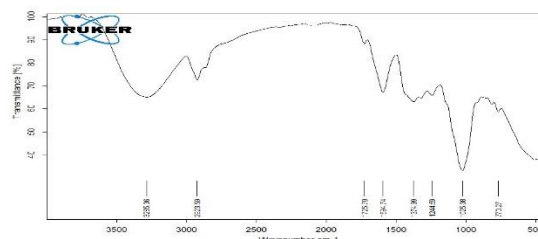


Figure 2: Infrared spectrum (IR) of banana peel.

Mineral analysis was determined using X-ray fluorescence (XRF) as illustrated in the experimental section. The obtained mineral content is presented in Table 5. It shows the concentration of potassium to be highest at 2.32 mg/g. The concentration (mg/gm) of calcium, magnesium, iron, and silicon were 0.106, 0.42, 0.046, and 0.241 respectively. The appreciable high content of potassium signifies that the peel is an important source of potassium. On the other hand, the banana peel under investigation is rich with a chlorine content of 0.75. The concentrations of the non-essential minerals of chromium, bromine, rubidium, strontium, zirconium, manganese, and Rubidium were found to range between 0.001-0.009 mg/100g. The result reveals that the banana peel contains very low concentrations of non-essential minerals.

**Table 5: Mineral analysis of banana peel**

Compound	m/m%	StdErr%	Element	m/m%	StdErr%
$\text{K}_2\text{O}$	2.79000	0.08000	K	2.32000	0.07000
Cl	0.75100	0.03700	Cl	0.75100	0.03700
MgO	0.69000	0.28000	Mg	0.42000	0.17000
$\text{SiO}_2$	0.49400	0.02400	Si	0.23100	0.01100
CaO	0.14900	0.04300	Ca	0.10600	0.03100
$\text{Fe}_2\text{O}_3$	0.06630	0.00330	Fe	0.04640	0.00230
$\text{Cr}_2\text{O}_3$	0.01130	0.00060	Cr	0.00770	0.00040
Br	0.01080	0.00050	Br	0.01080	0.00050
$\text{Rb}_2\text{O}$	0.01050	0.00060	Rb	0.00960	0.00060
SrO	0.00700	0.00030	Sr	0.00590	0.00030
MnO	0.00650	0.00060	Mn	0.00500	0.00050
NiO	0.00580	0.00030	Ni	0.00460	0.00020
$\text{MoO}_3$	0.00290	0.00030	Mo	0.00190	0.00020
ZnO	0.00210	0.00010	Zn	0.00170	0.00010

#### 3.2.2. Topography of BP and DBP

Further investigation of banana peel (BP) before and after deep drying (DBP) was carried out by SEM analysis to identify the development in their surface texture. Different representative areas with different magnifications were taken to show the most important texture. Microscopic and histochemical examination of banana peel. Photos A and C in Figure 3 show the

samples before drying, while photos B and D depict them after drying. It clearly shows the diversity of wall cell tissue types obtained and observes the primary surface walls of peel are markedly susceptible to interact leading to forming smooth surface tissues as clearly in photos B and D compared with photos A and C are compact tissues. Therefore, the chemistry of the upper surface can alter during the thermal drying of banana



peels, affecting the rate and degree of degradation. It is possible to draw the conclusion that thorough drying banana peels sufficiently will improve their degradability and break the lignin-carbohydrate complex (content of cellulose and hemicellulose); Furthermore, it may lead to a partial breakdown of the lignin macromolecule, resulting in a smooth and brittle texture for the finished product. This is why using it as a filler and thickening agent for the biogrease under study would be a good idea.

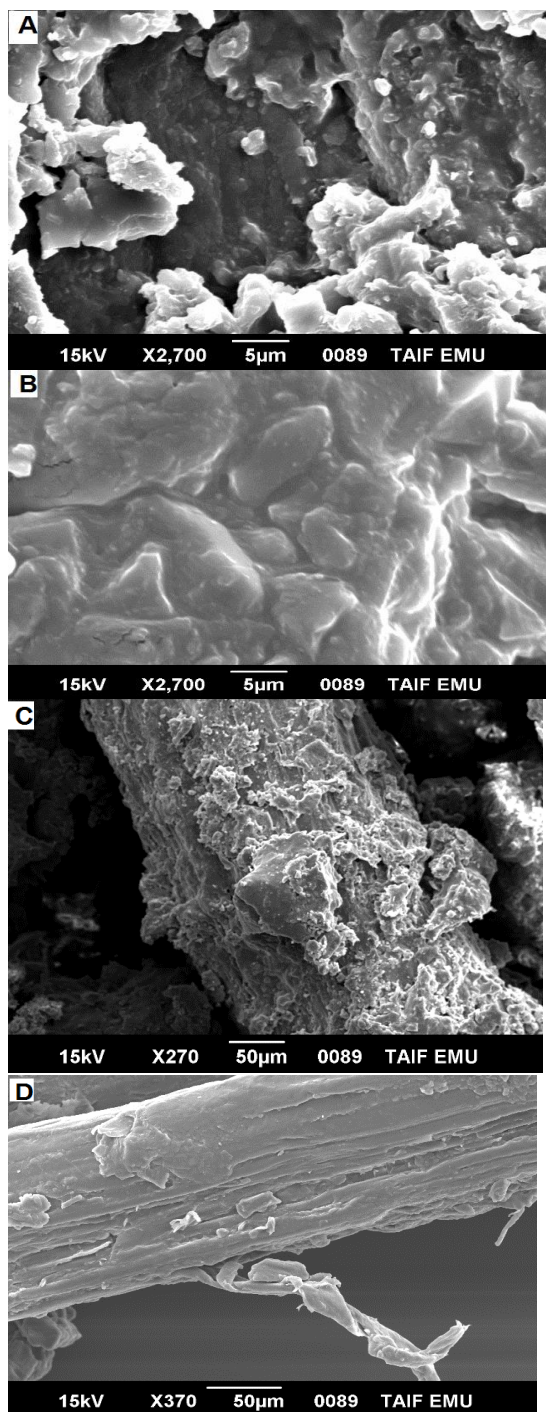


Figure 3: SEM micrographs of BP photos A, C and DBP photos B, D.

### 3.2.3. Thermal analysis

Thermogravimetric analysis (TGA) sheds light on the quantification of any change resulting from a transition. The results of the thermogravimetric examination of the thermal characteristics of the banana peel at a temperature range of 0-800°C are displayed in Figure 4. It shows that the pyrolysis of BP happened in three stages. Dehydration of the BP took place in the initial phase at temperatures between 50 and 200°C. The removal of the sample moisture content in this phase led to a weight reduction. Devolatilization or heat degradation of the organic components therefore took place in the second phase. The volatile matter content, which included the hemicellulose, cellulose, and lignin fractions, was decreased in this way. The third phase was characterized by low weight. This phase represents the formation of ash, which starts to form a steady state at temperatures ranging from 600-800°C. Also, the differential thermal analysis curve as shown in Figure 4 observed three endothermic reactions at 200, 400, and 600°C. As a result of various physical and chemical bonds breaking and/or forming at high temperatures, heavier reaction products, or the development of volatile chemicals, it is revealed that weight changes are a result of these processes. At temperatures between 600°C and 800°C, a steady state for the BP, which represents the ash content, was observed.

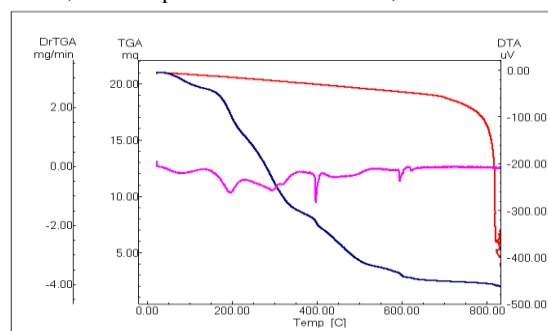


Figure 4: Thermogravimetric Analysis (TGA) and Differential Thermal Analysis (DTA) plots of banana peel.

### 3.2.4. Kinetic analysis

Kinetic parameters of thermal degradation of banana peel based on obtained TGA data to get a rough sense of the apparent activation energy are employed, following a solid-state reaction of thermal reaction occurs during TGA as mentioned in Figure (4). Equation (1) states that the rate depends on the degree of conversion:

$$\alpha = \frac{m_0 - m_t}{m_0 - m_f} \quad (1)$$

Where  $m_t$  is the mass at every time  $t$ ,  $m_f$  is the final mass, and  $m_0$  is the initial mass. Equation (2) can be used to describe the basic degradation kinetics equation.

$$\frac{d\alpha}{dt} = k(T)f(\alpha) \quad (2)$$

Where conversion and the temperature function, respectively, are denoted by:  $f(\alpha)$  and  $k(T)$ , respectively.  $K$  is the temperature-dependent reaction constant, and the Arrhenius equation, which is provided by Equation (3), defines it as follows:

$$k = A \exp\left(-\frac{E}{RT}\right) \quad (3)$$

Where A, T, R, and E stand for, respectively, the preexponential factor, absolute temperature, universal gas constant, and process activation energy. Equation (4) is formed by rearranging Equation (2) after substituting Equation (3) for Equation (2):

$$\frac{d\alpha}{dt} = A \exp\left(-\frac{E}{RT}\right) f(\alpha) \quad (4)$$

Equation (5) states that in the non-isothermal scenario, a heating rate (q) is used to increase the temperature.

$$\frac{dT}{dt} = q = \text{constant} \quad (5)$$

Consequently, Equation (6)

$$\frac{d\alpha}{dt} = \frac{A}{q} \exp\left(-\frac{E}{RT}\right) f(\alpha) \quad (6)$$

We employed the Kissinger-Peak technique [25], which makes the supposition that the peak temperature ( $T_p$ ) derived from the DTG corresponds to the maximal reaction rate. Equation (7), which represents the Kissinger-Peak equation [26], reads as follows:

$$\ln \left[ \frac{\beta}{T_p^2} \right] = \frac{E}{RT_p} + \ln \left[ \frac{AR}{E} \right] \quad (7)$$

A straight line is produced by plotting  $\ln(\beta/T_p^2)$  versus  $1/T_p$ . The activation energy (E) can be calculated from this line's slope.

The modelistic approaches use -temperature curves to fit and test the models while also determining the activation energy E, pre-exponential factor A, and mechanism n of the reaction. The relationship between the conversion function  $f(\alpha)$  and the reaction mechanism for a solid-state reaction is shown by Equation (8). This conversion function can be used to determine the reaction mechanism via the model-free method.

Where the empirically obtained exponent factors m, n, and p are used to ensure that one of them is always zero [27,28]. The final form is integrated to produce the following Equation (9) after the values in Equation (8) have been substituted and the variables have been separated. The explicit representation of the mechanism,  $g(\alpha)$  is shown on the left-hand side of the equation, which was created by integrating the conversion function of  $f(\alpha)$ . Using an approximative expression, activation energy was predicted using the Coats and Redfern calculation approach [28]. Equation (4), which takes the maximal reaction rate into account, results in Equation (10). The subscript 'max' designates the variables with the fastest rate of reaction. Additionally, when Equation (9) and Equation (10) are coupled, the resulting Equation (11) .

$$f(\alpha) = \alpha^m (1-\alpha)^n [-\ln(1-\alpha)]^p \quad (8)$$

$$\int_0^\alpha \frac{d\alpha}{\alpha^m (1-\alpha)^n [-\ln(1-\alpha)]^p} = \frac{A}{q} \int_0^T \exp\left[-\frac{E}{RT}\right] dt \quad (9)$$

$$\frac{1}{\frac{df(\alpha)}{d\alpha}} = - \frac{1}{f(\alpha_{\max})} \frac{A}{q} \frac{RT^2}{E} \exp\left[\frac{E}{RT_{\max}}\right] \quad (10)$$

Equation (10) can be used to obtain the size of the max, which can then be used to classify the kinetic models. For the current study, the non-isothermal modelistic approach developed by Coats and Redfern was used. The kinetic parameters, which range from 0.1 to 0.6, are determined using the data set obtained from the TG and DTG curves. The updated Coats and Redfern Equation (12) is shown below and can be used to get the kinetic parameters.

$$g(\alpha_{\max}) f(\alpha_{\max}) = -h \left[ \frac{E}{RT_{\max}} \right] \quad (11)$$

$$\ln \frac{g(\alpha)}{T^2} = \ln \left[ \frac{AR}{qE} - \frac{E}{RT} \right] \quad (12)$$

Where: A function and integral of  $f(\alpha)$ ,  $g(\alpha)$  is affected by the kinetic model of the reaction that is taking place. From Equation (12), a straight line is produced when  $\ln[g(\alpha)/T^2]$  is plotted against  $1/T$ . Its slope and intercept are E for the activation energy and A for the pre-exponential component, respectively. The algebraic formulation for the functions  $g(\alpha)$  will be determined by the mathematical model and conversion process [24,28]. When adopting modelistic techniques, the coefficient of linear regression (R2) frequently plays a key role in choosing the best reaction mechanism.

Additionally, it is advised that you compare the activation energies determined using modelistic and model-free methodologies to determine which mechanism works better. The results showed that when the values of E grew [24,28-32]. Here, we attempted to predict the outcomes individually for each kinetic parameter. The output parameters were the kinetic triplets of mechanism (n), activation energy (E), and pre-exponential factor (A). MATLAB was used to create the model. Data from a non-isothermal kinetic assessment of the prepared biogrease from used banana peels and cooking oil agreed with the studied kinetic model. In this respect, the input variables of the degree of conversion ( $\alpha$ ), the equivalent temperature in K, and the heating rate-based duration at minutes 5, 10, 15, 20, and 25°C min<sup>-1</sup> were explored as shown above in kinetic model and presented in Figures (5-7). The degree of conversion ( $\alpha$ ) from these figures has indicated 12 to 60% with a variation of 5%. The obtained data of the coefficient of linear regression (R<sup>2</sup>) from the experimental and the predicted values as shown in Figures (5-7), revealed somewhat close to 1. The projected output of an artificial neural network (ANN) was compared to the experimental values of E, ln A, and n with a coefficient of correlation that was shown near 1 as indicated in Figures (5-7).

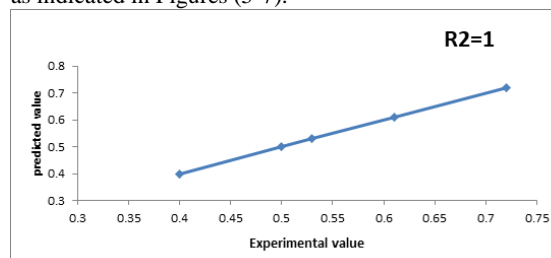


Figure 5: Comparison of the experimental E values with the predicted E values (ANN).

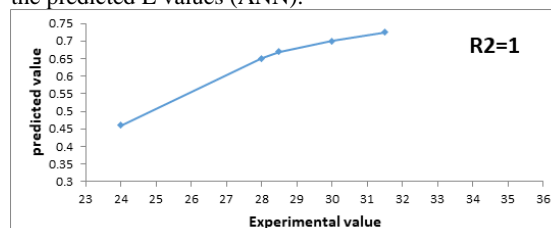


Figure 6: Comparison of the experimental lnA values with the predicted lnA values (ANN).

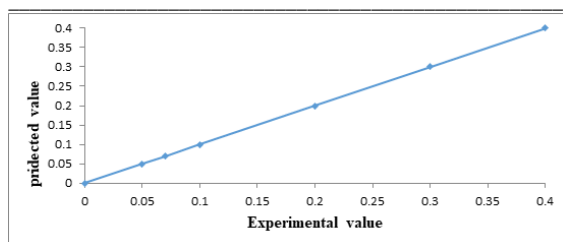


Figure 7: Comparison of the experimental n value with the predicted n values (ANN).

Input factors' respective proportional (%) effects on the outcomes E, ln A, and n were shown in Table 6. The selected time as the input variable was comparable with all the kinetic characteristics. On the other hand, the second most important factor determining the kinetic parameters was found to be temperature. The system cannot be considered spontaneous, it can be inferred. On the other hand, the kinetics of the thermal degradation of banana peel revealed that the experimental and predicted values were close to 1. This confirms that the banana peel acts as a thickening and filling agent for the obtained biogrease.

**Table 6: Relative importance of input variables on the output Kinetic parameters**

Kinetic parameters	Time (min)	Temperature (K)	Conversion (%)
lnA	43.17 %	36.56 %	24.08 %
E	45.5 %	42.57 %	18.91 %
n	48.05 %	29.89 %	27.35 %

### 3.3. Evaluation of the prepared bio-greases

In order to assess the effect of PWCO and DBP, five formulated biogreases under inquiry were prepared based on the component % shown in Table 1 in the experimental section; these greases are designated G1, G2, G3, G4, and G5 and compared with lithium commercial grease is designated G6. Experimental data reported in Table 7, show that the results of the physicochemical properties including penetration, oxidation stability, total acid number, dynamic viscosity, dropping point, and volume wear loss for the obtained biogreases G1, G2, G3, G4, G5, and G6. These greases clearly can be classified as general purpose industrial and automotive NLGI 2 grease based on the obtained penetration data worked and unworked. This reveals that the greases G1 to G5 based on the percentage (w/w) of lithium soap, PWCO, and DBP were crucial in determining the consistency or penetration values of the biogrease. They are prepared to have the penetration values in the range 260 to 294 as shown in Table 7. It clearly that the optimum ratio of DBP 20% to 30% was required to form biogrease with a stable texture and structure; also, it indicates that the DBP acts as a thickening agent and reduce the proportion of lithium soap needed to adjust the consistency of the prepared biogrease. In addition, the PWCO could diffuse and penetrate freely through DBP tissues which leads to improved physicochemical characterization of the prepared biogrease.

This finding is in agreement with earlier reports showing that grease preparation with suitable consistency needs a good selection of ingredient components [4,33]. It may be

concluded that the DBP acts as a thickening and filling agent for the obtained biogrease. On the other hand, Oxygen pressure drop data presented in Table 7, give an overview of the role of lignocellulosic compounds in controlling the oxidation reactions. The data indicates that the biogreases that were synthesized had an oxidation inhibition efficiency in the following order: G5 > G4 > G3 > G2 > G1. This could be explained by the polyphenolic ingredient of lignin, which undergoes extensive conjugation and contributes to stabilizing the free radical produced by the oxidation reaction. This illustrates DBP's function in considering a possible antioxidant source for produced biogreases.

This is consistent with findings that evaluated the antioxidant qualities of banana peels [34]. Experimental data concerning the dropping point of prepared biogreases are listed in Table 7. It shows that increasing the DBP ratio increases thermal stability and dropping points. This is attributed to some interactions between lignocellulosic compounds and fatty compounds including inter- and intra-molecular hydrogen bonding leading to fortifying the binding forces between ingredients (lithium soap, PWCO, and BP) which promotes the production of reinforcement grease texture. This interpretation agrees with the data on penetration values.

Careful inspection in Table 7 shows improvement and reinforcement in all physical and chemical characteristics that affect the consistency, dropping point, penetration, and oil separation of prepared grease, especially, for G3, G4, and G5. It confirmed that the development of biogrease with proper consistency requires a strict improvement of the components and the preparation system. On the other hand, the obtained results indicate that biogreases G3, G4, and G5 are more efficient compared with G1 and G2. This is attributed to the ability of the lignocellulosic compounds to fortify the binding force with the soap texture.

Also, the thickening power of these compounds modifies the grease backbone and improves the thermal and mechanical stabilities. It could explained that based complex chemical composition of banana peel leads to an increase in the consistency of the waste cooking oil with lithium soap thickener. It was concluded that the greases had satisfactory performance in most automotive applications NLGI 2. On the other hand, by comparing the wear properties of the prepared biogreases and the commercial ones, it is found that the volume wear loss decreases in the following order G5 > G4 > G1 > G3 > G2 > G6. This reveals that commercial grease G6 has the lowest volume wear loss compared with all prepared biogreases. This is probably due to the lack of adsorption of prepared biogreases with the surface pin. Accordingly, this work will needed to add some antiwear additives in future work.



**Table 7: Physicochemical properties of prepared biogreases G1-**

Test	Prepared biogreases						Test method
	G1	G2	G3	G4	G5	G6	
Penetration at 25°C							
Unworked	295	290	285	275	260	270	ASTM D-217
Worked	294	293	285	275	260	272	
Dropping point, °C	135	140	150	165	190	190	ASTM D-566
TAN, mg KOH/gm,at72h	0.1	0.1	0.1	0.1	0.1	0.1	ASTM D-664
Oil separation, Wt%	1.5	1.1	0.4	0.3	0.3	0.1	ASTM D-1724
Oxidation Stability at, 99°C, 96h, pressure drop, psi	5.1	4.9	3.5	3.2	3.1	5.8	ASTM D-942
Copper Corrosion 3h/100°C	Ia	Ia	Ia	Ia	Ia	Ia	ASTM D-4048
Volumetric wear loss, mm3	0.7	0.8	0.9	0.9	1.0	0.3	ASTM G 99-05

### Conclusion

1. Waste cooking oils containing a high percentage of myristic and palmitic acids are good fluids for preparing biogreases
2. The chemical analysis of the banana peel under investigation gives a good idea of the lignocellulosic compounds which have an important role as a thickening agent for biogrease. Replacing the lithium stearate soap (stearic acid, lithium hydroxide) thickener with cheaper alternative agricultural substrates BP, will save production costs.
3. The prepared biogreases under investigation have NLGI 2 according to international classification and have outstanding resistance to oxidation
4. In general, the prepared biogreases have physicochemical properties similar to those found in commercial ones except for the wear properties and the introduction of purified waste cooking oil and banana peel in biogreases enhances the economic and environmental aspects.

### References

1. H. J. Bernard, S.R. Schmid and B.O.Jacobson, "Fundamentals of fluid film lubrication". 2nd Ed. New York: Marcel-Dekker,(2004).
2. J. Harris, "History and Current Status of NLGI Reference Greases", NLGI Spokesman 59 Vol. 12, pp.18 – 22, (1996).
3. L.A.T. Honary, "A study of compatibility of fully formulated biobased and conventional greases", NLGI Spokesman., Vol. 75, pp. 20, (2011).
4. R.A. El-Adly, "Producing multigrade lubricating greases from animal and vegetable fat by products". Journal of Synthetic lubrication, Vol.16, pp.323–332, (2000).
5. R.A. El-Adly and E. A. Ismail. "Lubricating greases based on fatty by-products and jojoba constituents", Tribology-lubricants and lubrication, (2011)
6. R.A. El-Adly, S.M. , El-Sayed and M.M. Ismail; " Studies on The Synthesis an Utilization of Some Schiff's Bases: 1. Schiff's Bases as Antioxidants for Lubricating Greases"J. Synthetic Lubrication Vol.22, pp. 211-223,(2005).
7. S. Z. Erhan, B. K. Sharma, and J. M. Perez, "Oxidation and low temperature stability of vegetable oil-based lubricants," Industrial Crops and Products, vol. 24, pp. 292-299, (2006).
8. H. A. Abdulbari,, M. Y, Rosli,. H. N. Abdurrahman and M. K. Nizam,, "Lubricating grease from spent bleaching earth and waste cooking oil: Tribology properties", International Journal of the Physical Sciences Vol. 6(20), pp. 4695-4699, (2011).
9. L.A.T. Honary and R. Erwin., "Biobased lubricants and greases", chemistry, technology and products, Ltd (2011).
10. A. K. Bhatnagar, S. Kaul, V. K. Chhibber and A. K. Gupta, "HFRR Studies on Methyl Esters of Nonedible Vegetable Oils" Energy Fuels, vol.20,pp. 1341-1344,(2006).
11. J.Porwal, P. K. Khatri, S. Kaul, B. Behera, N. Atray and S. L. Jain "Polymer-grafted sulfonated carbon-catalyzed synthesis of  $\alpha$ -hydroxy ethers as biolubricants from waste vegetable oil". Biomass Conversion and Biorefinery (2020).
12. P.D. Patil, V.G. Patil and S Deng,. "Biodiesel production from jatropha curcas, waste cooking, and camelina sativa oils". Industrial & Engineering Chemistry. Vol.48 pp.10805–10850.
13. N. Singh, P. Agarwal and S. K. Porwal "Natural Antioxidant Extracted Waste Cooking Oil as Sustainable Biolubricant Formulation in Tribological and Rheological Applications". Waste and Biomass Valorization, Vol.13 pp.3127–3137, (2022).
14. Fao. "Banana Fusarium Wilt Tropical Race 4: A mounting threat to global banana markets?" (November) (2019).
15. A. Ferrante, C. Santulli and J. Summerscales "Evaluation of tensile strength of fibers extracted from banana peels". Journal of Natural. Fibers Vol. 17 (10), pp.1519–1531.(2019)
16. S.Arya ,K.Ankeeta and J. Waghmare "Utilization and application of banana peel". Food Market Technol. (JANUARY): 2 (2015).
17. S. M. Kumar, T., N. Rajini, A. Alavudeen, S. Siengchin, V. Rajulu, and N. Ayrilmis. "Development and analysis of completely biodegradable cellulose/banana peel powder composite films". Journal of Natural Fibers, Vol. 18, No. 1, pp. 151–160 (2019).
18. A.M. Shoaib , R.A. El-Adly , M.H.M. Hassanean , A. Youssry and A.A. Bhuran "Developing a free-fall reactor for rice straw fast pyrolysis to produce bio-products", Egyptian Journal of Petroleum, Vol. 27, pp. 1305–1311, (2018).



19. K. Warner, "Chemistry of frying oils". In Food lipids, CRC Press, pp. 222-239,(2002). Polonorum Technologia Alimentaria Vol.6(3) (2007)
20. M.A. Dalia, "A study on preparation and evaluation of thread grease from renewable resources" Ph.D. Ain Shams University (2023).
21. A.O. Ayeni, O.A. Adeeyo, O.M. Oresegun and T.E. Oladimeji "Compositional analysis of lignocellulosic materials: Evaluation of an economically viable method suitable for woody and non-woody biomass"; American Journal of Engineering Research Vol. 4(4) pp. 14-19, (2015).
22. R.A. El-Adly1, M. Adel Yossef, Enas A. Ismail, Modather, F. Hussein, Dalia M. Abbas, "Biogrease Based on Biochar from Rice Straw and Waste Cooking Oil", International Journal Of Advances In Pharmacy, Biology And Chemistry vol.4(1),(2015).
23. C. Avisha, M. Debarati, and B. Dipa; "Synthesis of Biolubricant Components from Waste Cooking Oil Using a Biocatalytic Route". Environmental Progress & Sustainable Energy, vol.33, pp. 933-940, (2014).
24. H. E. Kissinger, "Reaction kinetics in differential thermal analysis", Analytical. Chemistry. Vol. 11, pp. 1702–1706, (1957).
25. L. T. Vlaev, V. G. Georgieva and S. D. Genieva,, "Products and kinetics of non-isothermal decomposition of vanadium(IV) oxide compounds", Journal of Thermal Analysis and Calorimetry . Vol.88, pp.805–812, (2007).
26. K.Chrissafis, "Complementary use of isoconversional and model-fitting methods", Journal of Thermal Analysis and Calorimetry. Vol.95, pp. 273–283, (2009).
27. L. T. Vlaev, V. G. Georgieva and S. D. Genieva "Products and kinetics of non-isothermal decomposition of vanadium(IV) oxide compounds", Journal of Thermal Analysis and Calorimetry Vol.88, pp.805-812, (2007).
28. J.Šesták, and G. Berggren "Study of kinetics of the mechanism of solid-state reactions at increasing temperatures", Thermochemica Acta, Vol. 3 (1), pp.1-12, (1971).
29. C.M. Andrea; G. B.-Peñafiel, M. A.Aguiar, G.G.-Vinueza and C. M. Calderón "Devolatilization as an alternative for energy valorization of bio-medical waste: kinetic study". revista. ion. Vol.35(2)pp.49-58 (2022).
30. A. Starón. "Composite Materials Based on Waste Cooking Oil for Construction Applications". Buildings, Vol. 13 p. 994 (2023).
31. T. Itoh , K. Iwabuchi and K. Ota "A new approach to stabilize waste biomass for valorization using an oxidative process at 90 °C" ,plos one. (2018).
32. R. N. Sarma and Vinu, R. "Current Status and Future Prospects of Biolubricants: Properties and Applications" Lubricants, Vol.10 (4) p.70 (2022).
33. M. I. Al-Wakeel and R. A. El-Adly "A Novel Application of Egyptian Oil Shale as a Filler in the Production of Lithium Lubricating Grease", Energy Sources, Vol. 27(16), pp.1511-1522. (2005).
34. D. Chodak and T.Tarko "Antioxidant Properties Of Different Fruit Seeds And Peels", Acta Scientiarum